Sub-severe and Severe Hail

2	Kimberly L. Elmore, ^a John T. Allen, ^b Alan E. Gerard, ^c
3	^a Cooperative Institute for Severe and High-Impact Weather Research and Operations, The
4	University of Oklahoma, and NOAA//National Severe Storms Laboratory Norman, OK
5	^b Department of Earth and Atmospheric Sciences,
6	Central Michigan University, Mt. Pleasant, Michigan, USA
7	^c National Severe Storms Laboratory
В	National Atmospheric and Oceanic Administration, Norman, Oklahoma, USA

9 Corresponding author: Email: kim.elmore@noaa.gov

ABSTRACT: The occurrence and properties of hail smaller than severe thresholds (diameter < 25 mm) are poorly understood. Prior climatological hail studies have predominantly focused on large 11 or severe hail (diameter at least 25 mm or 1 inch). Through use of data from the Meteorological 12 Phenomena Identification Near the Ground project, Storm Data, and the Community Collaborative Rain, Hail and Snow Network the occurrence and characteristics of both severe, and sub-severe 14 hail are explored. Spatial distributions of days with the different classes of hail are developed on an 15 annual and seasonal basis for the period 2013-2020. Annually, there are several hail-day maxima that do not follow the maxima of severe hail: the peak is broadly centered over Oklahoma (about 28 days per year). A secondary maxima exists over the Colorado Front Range (about 26 days per 18 year), a third extends across northern Indiana from the southern tip of Lake Michigan (about 24 days per year with hail), and a fourth area is centered over the corners of southwest North Carolina, 20 northwest South Carolina, and the northeast tip of Georgia. Each of these maxima in hail days are 21 driven by sub-severe hail. While similar patterns of severe hail have been previously documented, 22 this is the first clear documentation of sub-severe hail patterns since the early 1990s. Analysis of the hail size distribution suggests that to capture the overall hail risk, each dataset provides a complimentary data source.

26 1. Introduction

In the United States, hail size is divided into two classes: severe, meaning a diameter of at least 27 25 mm (1") and sub-severe, meaning anything less than 25 mm diameter, but greater than the 5 mm diameter of graupel (Allen et al. 2020). These two size classes are used to define whether 29 the event meets severe criteria. Prior to January 2010, the severe class was defined as hail with 30 a diameter at least 19 mm (0.75 in). The overall occurrence of hail has been regularly explored in the United States given its substantive and rising impacts to both property and agriculture, however, how frequently smaller hail sizes occur has received less attention (Changnon 1999; Sander et al. 2013; Brown et al. 2015; Tang et al. 2019; Allen et al. 2020). Inferring the occurrence of hail is challenging owing to the spatial and temporal inhomogeneities that arise from typical observer-sourced datasets used to validate severe thunderstorm warnings (i.e. SPC Storm Data; Kelly et al. 1985; Schaefer et al. 2004; Doswell et al. 2005; Allen and Tippett 2015; Allen et al. 37 2017; Taszarek et al. 2020a). The relationship of these data to warning verification (Blair et al. 2011; Bunkers et al. 2020) means that size criteria within the dataset are mostly confined to no less than 19 mm (0.75 in) for hail and so sizes smaller that 19 mm are poorly represented. Smaller sizes are occasionally included if they are associated with severe wind, or a tornado. As noted by Changnon (1999), this limits the utility of these data in describing the true hail frequency, or the full distribution of hail sizes that occur. Only about the last two decades contain reliable hail 43 data (Allen and Tippett 2015) meaning that prior to the 1990, these data are rarely used because they lacked the necessary consistency to ascertain the true frequency of hail of any size in the United States (Changnon 1999). Instead, prior studies relied either on station-based observations (Changnon 1977; Changnon Jr 1977; Changnon and Changnon 1997, 2000; Changnon et al. 2001, 2009), hailpads, or agricultural damage data to infer these events. While these past datasets for the most part still exist for assessment of hail occurrence, station-based observations have only had size information for brief periods and formal observations were terminated in the 1990s. Hailpad records have generally been inconsistent in their maintenance or heavily regionalized (e.g. Reges et al. 2016), seriously limiting any climatological utility.

The limitations of Storm Data have spurred newer approaches that are more dynamic and widespread to collect precipitation data including hail. For example, the CoCoRAHS observation network collects more detailed hail information through either hail pads or spotter observations and

includes each of the smallest, average and largest size of hail along with other properties (Reges et al. 2016). Other high density observation collection efforts include the Severe Hazards and 57 Analysis and Verification Experiment (SHAVE, Ortega et al. 2009; Ortega 2018), which actively probed areas around strong storms in near-real time to obtain observations to verify temporal and spatial scales of hail for the verification of radar derived hail products. While an effective approach 60 to collate hail events, it was limited in coverage, and by the available personnel to make calls at 61 any given time. Despite these limitations, SHAVE documented otherwise unprecedented unknown scales of hail fall and size on a comparatively large sample of storms. In parallel there have also been small scale efforts to source high density measurements in the field, and while they have also 64 contributed to our understanding of hailstone and hail fall properties, their records are too sporadic to contribute to the climatological understanding (Blair et al. 2017; Giammanco et al. 2017). 66

A more accessible and easily managed approach to collating hail information has been through
the Meteorological Phenomena Identification Near the Ground (mPING) project that implements
a flexible Application Program Interface on a mobile phone platform to crowdsource volunteer
reports of precipitation events (Elmore et al. 2014). As a result of these efforts, the mPING project
has garnered an impressively large collection of hail events in the past 8 years across the continental
United States, ranging from 6.35 mm (0.25 in) maximum diameter through sizes in excess of 125
mm (5 in). By approaching the problem through this platform, mPING provides valuable insight
into the hail sizes that are not traditionally collected or sought by existing approaches. Despite
these favorable attributes, to date data from mPING have not been used in a climatological context,
and small hail climatology over the United States has not been explored since 2005 (Changnon
et al. 2009).

While a number of studies have explored the individual datasets that characterize hail occurrence (e.g. Changnon 1999; Doswell et al. 2005; Changnon et al. 2009; Allen and Tippett 2015; Grieser and Hill 2019), no effort has been made to explore a more comprehensive picture of hail occurrence through the synthesis of multiple observational datasets to leverage their relative strengths and address their weaknesses. This limitation to existing approaches has only been emphasized since the retirement of detailed hail reporting from station observations (Changnon 1999), leading to an incomplete picture of hail day occurrence for the full distribution of hail sizes. Understanding the climatology of all hail is important as sub-severe hail can lead to significant agricultural damage

(Changnon Jr 1971; Changnon and Changnon 1997), and if accumulated can result in dangerous road conditions and localized flash flooding (Kumjian et al. 2019; Friedrich et al. 2019). In some 87 regions and seasons, these smaller hail sizes can be the primary mode of occurrence (e.g. Miller and Mote 2017), and can provide important insights into ice processes of strong convective clouds (Van Den Heever and Cotton 2004; Kacan and Lebo 2019). The analysis of the spatial distribution 90 of all hail sizes is also essential for the cross-validation of proxy hail climatologies that are derived 91 through the use of remotely-sensed satellite and radar platforms (e.g. Cintineo et al. 2012; Cecil and Blankenship 2012; Bang and Cecil 2019; Murillo et al. 2021; Wendt and Jirak 2021). For example, using only SPC storm reports to validate these measurements, it is not clear whether the radarderived frequencies indicated from maximum expected size of hail detections (MESH, Murillo et al. 2021; Wendt and Jirak 2021) were an overestimate of hail frequency, or an overestimate of 96 hail sizes or perhaps a combination of both. To this end, in this paper we consider climatological 97 frequency and bulk statistics of hail as ascertained from the combination of mPING, Storm Data, and CoCoRaHS and explore the relative strengths and weaknesses of each dataset. The aim of this work is to produce a comprehensive climatology of hail in the contiguous Unites States and, 100 in so doing, recognize unique strengths and weaknesses of each data source and the information 101 provided through their cumulative hail observations.

2. Data and methods

Data used in computing hail days for sub-severe and severe hail come from two sources: the National Oceanic and Atmospheric Administration/National Centers for Environmental Information 105 (NOAA/NCEI) Storm Data publication and mPING. These two sources differ substantially in that 106 Storm Data is primarily used for NWS warning and verification purposes. This means that offices 107 actively probe for relevant reports in areas of suspected severe weather, and reporting in the vicinity 108 of NWS offices involves a higher fraction of NWS Employee reports (Allen and Tippett 2015). 109 Reports are entered as the nearest reference object identified by the user or NWS employee entering 110 the report. mPING in contrast is a passive collection of voluntarily provided reports provided by mPING users. Unlike Storm Data, users are also provided a referential list of hail sizes at quarter 112 inch intervals and associated reference objects, which may assist in mediating size clustering bias 113 toward known reference objects (Allen and Tippett 2015; Blair et al. 2017). The period of record

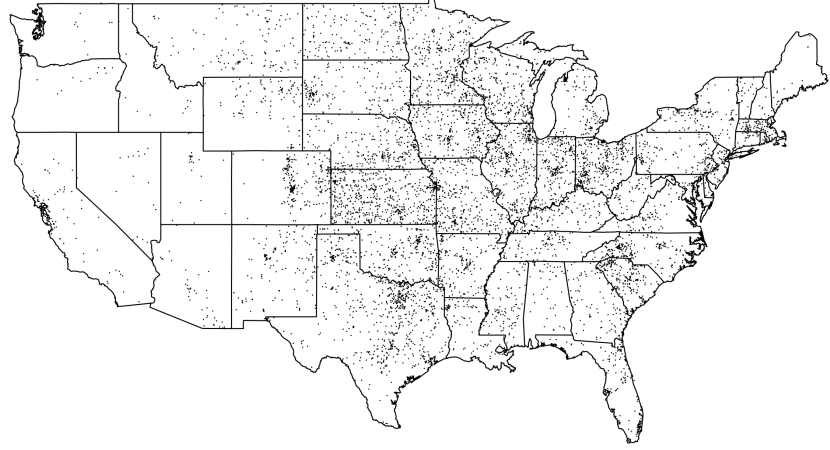
for mPING considered here spans eight years from 1 Jan 2013 through 31 Dec 2020, however, mPING remains operational.

The nature of mPING observations means that they are automatically located in space and 117 time by GPS and are thus spatially more accurate than other sources of reports, unless a user moves a considerable distance from the observation or waits a long time to send the report; 119 cursory examination shows no evidence of such. No quality control is performed to mPING 120 hail observations, outside of truly erroneous submissions, though no systematic biases that would 121 influence the study results are present to the authors' knowledge. Storm Data does not enjoy such 122 precision and while Storm Data errors have been well documented (e.g. Witt et al. 1998) here we 123 take several steps to address these potential sources of error on the derived climatology. One area 124 that cannot be remedied is the serious bias in hail size reports as sub-severe hail is not generally 125 recorded except in cases where it may be in association with another type of significant weather 126 (winds, tornadoes, etc.). In contrast, mPING encourages reports of sub-severe hail and so is the 127 only available data source for a more general all hail climatology. Both sources suffer from a spatial bias in that reports are naturally more numerous in and around population centers and road 129 networks (Allen and Tippett 2015). Without care, this can lead to misleading conclusions related 130 to the association of high frequency hail with high population density.

To illustrate these potential biases in the two datasets and the distinct difference in the raw frequency of reports, we consider both sub-severe (Figs. 1a,b) and severe (Figs. 2a,b) point clouds from Storm Data and mPING, respectively. In both figures, areas of higher report density are clearly associated with cities and metropolitan areas in hail prone regions. Such density variations are non-physical artifacts and therefore must be removed to the extent possible.

One approach to diminishing these population derived artifacts is through an analysis procedure that diffuses, filters, or "spreads out" this dependence over an appropriate area, an approach that has been used in numerous studies (e.g. Brooks et al. 2003; Gensini et al. 2020). Approaches such as Schaefer et al. (2004) treat this by aggregating (binning) Storm Data severe hail reports into 2 degree squares, averaging across the squares, then normalizing the results to reports per decade per $34,300 \ km^2 (10,000 \ nmi^2)$. Hexagonal binning (Carr et al. 1992) is another way to deal with this effect that has advantages over rectangular binning and therefore is the approach used here. Chiefly, hexagons are the most complex polygon that can be tessellated over a surface, and are

a) Storm Data Sub-Severe Hail 2013-2020



b) mPING Sub-Severe Hail 2013-2020

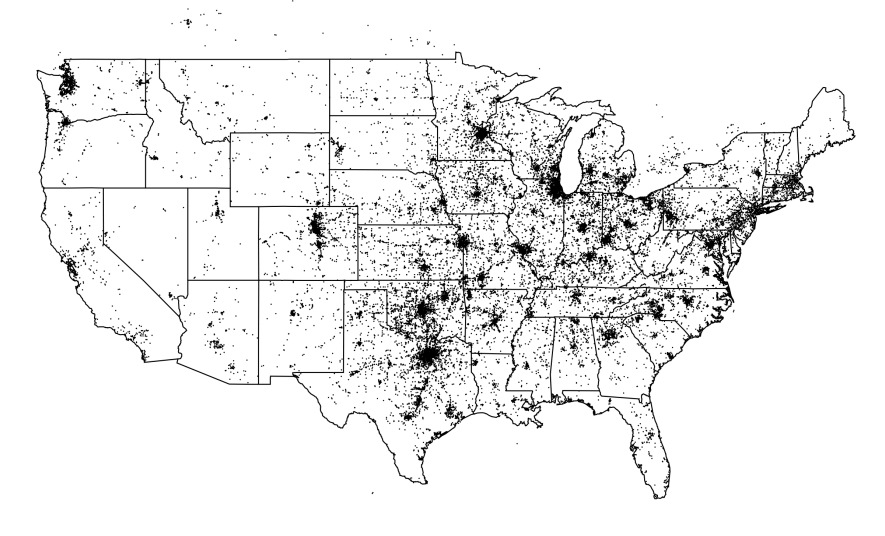
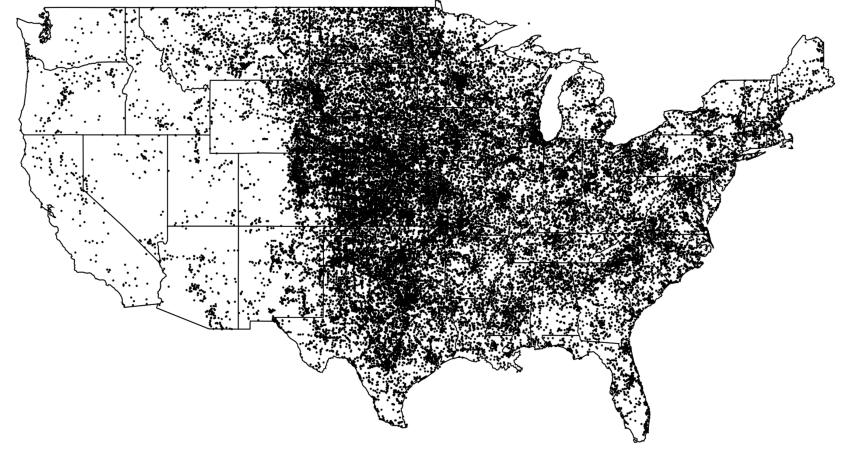


Fig. 1. a) Point cloud showing Storm Data reports of sub-severe hail spanning the period 1 Jan 2013 through 31 Dec 2020; each point represents the location of a single Storm Data report. b) Same as Fig. 1a, but showing sub-severe reports from mPING. .

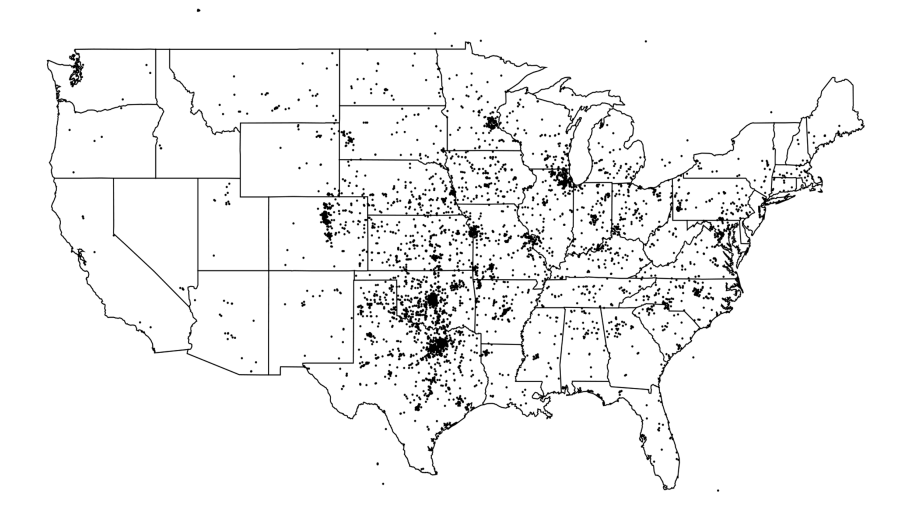
more similar to circles than are squares. Thus, hexagons and hexagonal binning constitute the most efficient and compact division of 2D data space. This property helps reduce the edge and border effects inherent in rectangular binning procedures.

For this work, a grid of 23 x 23 hexagons are distributed over the CONUS, providing for 529 center points. From this set, not all hexagons have hail observations as illustrated in Fig. 3. We experimented with the maximum number of hexagons, and found that the aforementioned grid provided was the highest resolution that could be used before population centers began to clearly

a) Storm Data Severe Hail 2013-2020



b) mPING Severe Hail 2013-2020



162

164

165

Fig. 2. a) Point cloud showing Storm Data reports of severe, as in Fig. 1a. b) As for Fig 2a, but for mPING reports of severe hail.

influence results. Each hexagon includes an area of about 32,600 km^2 (roughly equivalent to a 100 km radius circle). This area reflects a similar scale to that of Schaefer et al. (2004), thereby allowing for more direct comparison despite the different gridding approach.

To calculate the number of days with hail, reports from either dataset are binned within each hexagon; each day is counted only once. This step is critical to ensure that if there are many reports within a hexagon for a given date, that day is counted only once. Because the period of record covers eight years, the total number of days is divided by a factor of eight to yield the average number of hail days per year.

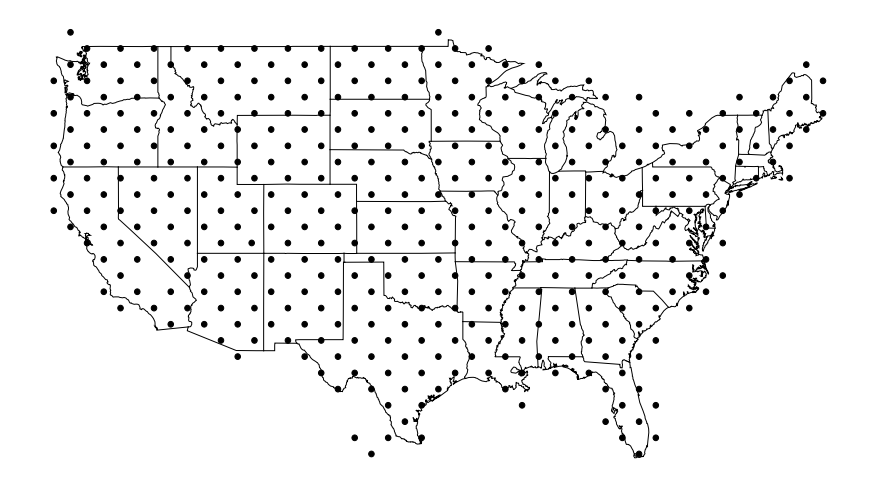


Fig. 3. Points showing the center of hexagonal cells that contain reports from either Storm data or mPING over the period 1 Jan 2013 through 31 Dec 2002.

To smooth the results from the original hexagonal grid, a local, quadratic least squares surface is fit to the resulting grid of counts as an additional smoothing step (LOESS Cleveland 1979; Cleveland and Devlin 1988). The resulting fit is applied to a finer grid for plotting purposes, and then used as the basis for contours of days per year of sub-severe hail, severe hail, or any hail.

Storm Data timestamps have known inaccuracies and tend to be biased late (after the event), yet Storm Data report time errors seldom exceed 1 hour (Witt et al. 1998). Provided that mPING users submit reports during or very shortly after an event, mPING reports have reduced time errors relative to Storm Data. Times from both source datasets are used to generate distributions of event times, in local solar time (LST), to evaluate the most common time of day for hail events and to discern whether any difference exists between times by season or hail size. Occurrence time distributions are then estimated using kernel density estimates computed at 201 points each using a Gaussian weighting 12.7 mm wide (0.5 in) truncated at four standard devaitions (KDEs, Silverman 1998).

Finally, a third data source reflecting the next largest available dataset was also considered, the Community Collaborative Rain, Hail and Snow Network (CoCoRaHS Reges et al. 2016). As time information from CoCoRaHS is unreliable and difficult to ascertain, we instead focus on its application for understanding hail size distributions. We use CoCoRaHS to help generate distributions of hail size and estimate the proportions of sub-severe and severe or larger hail.

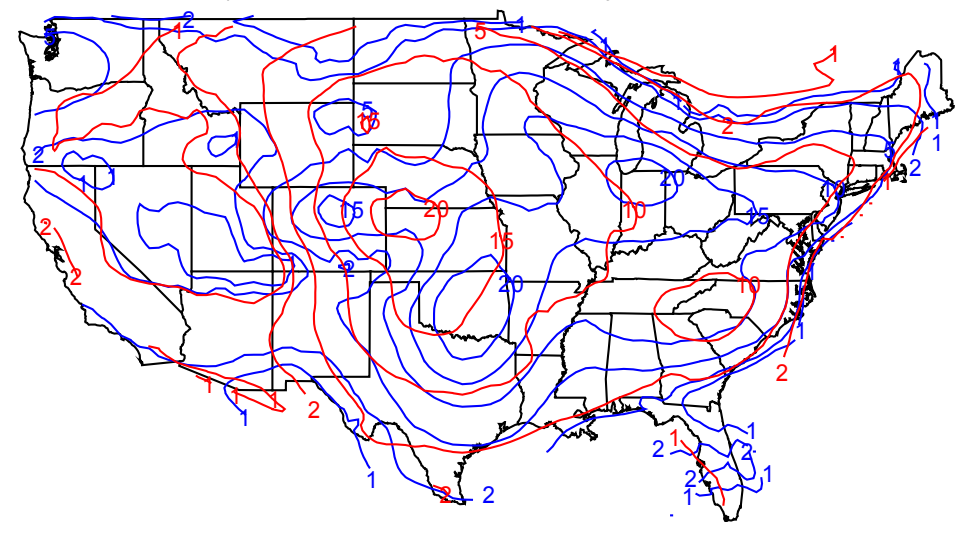
For this application the use of both CoCoRaHS and mPING allows for a more comprehensive viewpoint of sub-severe hail, as Storm Data does not provide sufficient data of this type. The resulting distributions are created through empirical cumulative density functions (eCDFs).

8 3. Results

a. Sub-severe and Severe Hail Frequency

Here we compare and contrast both the common and complimentary qualities of Storm Data and 190 mPING for severe and sub-severe hail days. Unsurprisingly, there is a much larger fraction of sub-191 severe reports within mPING, and severe or greater reports in Storm Data (Figs. 1, 2), suggesting that these two datasets are likely complementary by providing insight into different sizes of hail, 193 rather than one being notionally superior to the other. Following gridding and smoothing to the 194 annual average number of hail days of any size, Fig. 4 shows an estimate of the average total number of days with any hail across the CONUS as estimated using Storm Data (red) and mPING (blue). This approach further illustrates the differences between the two datasets because any hail 197 frequency illustrates regions where hail less than an arbitrary size threshold often occurs. This is particularly evident over the western U.S. where larger hail sizes are comparatively rare (Schaefer et al. 2004; Allen and Tippett 2015). Higher frequencies are particularly evident outside of the 200 typical Great Plains severe hail maxima, with higher frequency on and near the foothills of the 201 Rocky Mountains, over the Midwest and East. Combining the two datasets however, provides a complementary picture of the total number of hail days. We expect that the values in Fig. 4b 203 provide the most accurate representation of average yearly hail days across the CONUS. These 204 values are more broadly consistent than long term hail data records based on station data, though with some differences, including slightly higher frequencies reflecting the broader spatial sampling 206 (Changnon and Changnon 2000). For example, Changnon and Changnon (2000) reported a hail day 207 frequency of 21 for Denver, CO, and Dodge City, KS, with a gradient through eastern KS. However, 208 over regions with more sparse population, the reliability of observation stations overshadows this benefit. It is important to note that these sources are not exclusive or independent: a day that counts 210 as a sub-severe hail day may also count as a severe hail day and vice versa. This explains why Fig. 211 4b is not simply the simple sum of occurrences within Storm Data and mPING.

a) Storm Data and mPING Hail Days 2013-2020



b) Combined Storm Data and mPING Hail Days 2013-2020

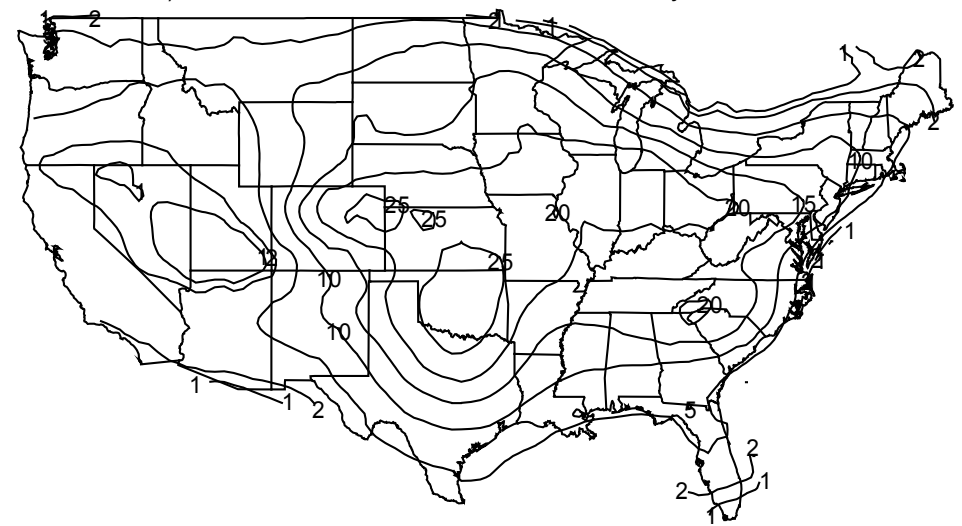
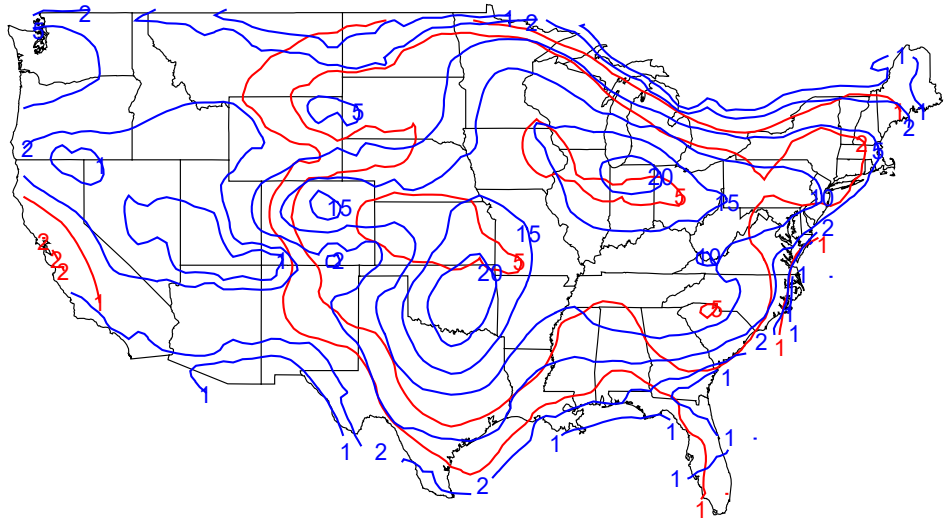


Fig. 4. a) Contours of the average number of hail days per year for hail of any size from Storm Data (red) and mPING (blue). b) As for a) but for combined Storm Data and mPING reports.

Spatially, the overall patterns are similar to Schaefer et al. (2004), however, we note that study provides contours in number of *reports* per 10 years and thus the results are not directly comparable. The overall frequency of that study also depicts a maximum number of reports to be nearly 60 per year for hail exceeding 0.75 in. This number is well in excess of the nearly 30 per year for any hail size shown in Fig. 4b, reflecting the difference obtained if an approach uses hail *days* rather than hail *reports* (Doswell et al. 2005; Allen and Tippett 2015). For this reason, in this work any single day that receives n>1 reports still counts as a single day within a hexagonal bin.

a) Storm Data and mPING Sub-Severe Hail Days 2013-2020



b) Combined Storm Data and mPING Sub-Severe Hail Days 2013-2020

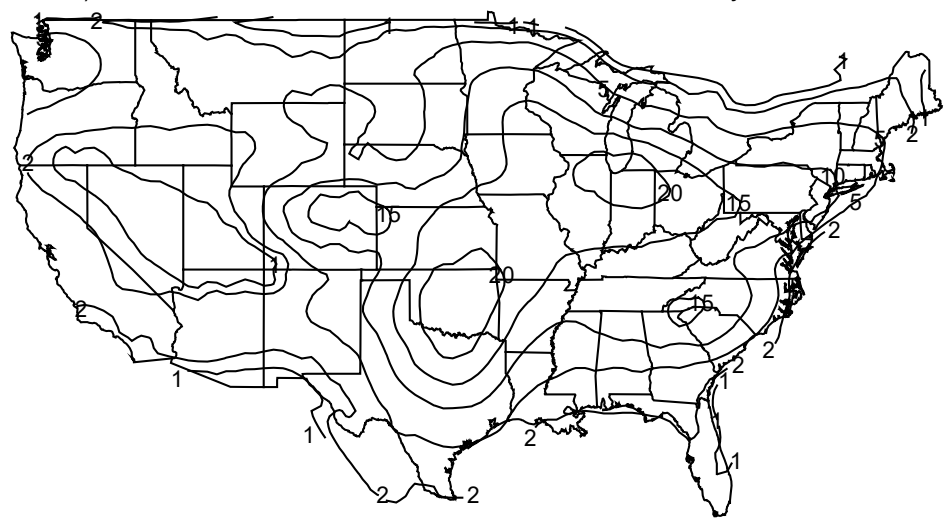


Fig. 5. a) Contours of the average number of hail days per year for hail of sub-severe size from Storm Data (red) and mPING (blue). b) As in Figure 5a, but for combined reports from both Storm Data and mPING.

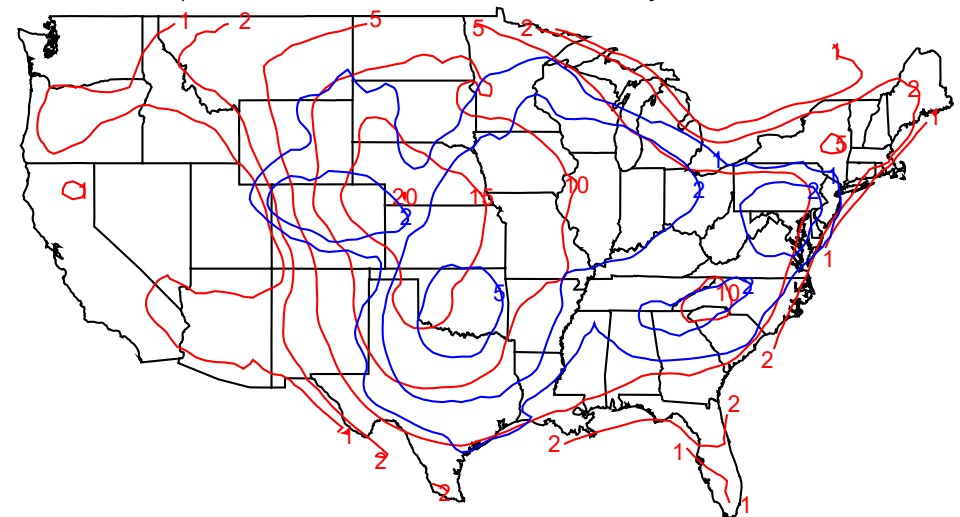
Sub-dividing these reports into mean sub-severe days per year only, the differences between the two datasets are further emphasized (Figs. 5a and b). Storm Data shows two maxima, one of 6-7 days per year across NW KS and another near Charlotte, NC. However, this is clearly an under-representation of the true frequency, as mPING shows what is almost certainly a more accurate depiction of sub-severe hail days because mPING is not, by design, biased towards severe hail. The most significant differences are in regions outside the traditional 'hail belt', with maxima in the Colorado Front Range, central OK, and also an E-W region encompassing parts of the lower

midwest, as well as KY, NC, SC, GA and northeast AL. Curiously, the frequency of mPING reports 231 also introduce spatial inhomogeneities, for example Storm Data reports are more likely across the 232 California seaboard as compared to those from mPING. In combining the two datasets (Fig. 5b), 233 these reports show a pattern with clear maxima (24 days) over central OK, a NE-SW band from S WI into N OH touching the S tip of Lake Michigan (18-24 days), a clear separate maximum 235 along the front range of the Rocky mountains extending into E CO (16 days), and finally a fourth 236 maximum encompassing E KY, the SW corner of NC, the NW corner of SC, N AL and N MS 237 (14-16 days). The maximum in C OK is part of a general ridge of high sub-severe hail frequency 238 that extends into the Great Lakes region. 239

The patterns for severe hail (Figs. 6a and b) are decidedly different from sub-severe hail, and 240 while spatially consistent are higher in frequency than the hail day rate reported using Storm 241 Data alone (Allen and Tippett 2015), likely reflecting continual growth in hail reporting frequency. 242 Storm Data shows a maximum of 20 days at the junction of NE-KS-CO, along with a broader region 243 of active severe hail days extending into W NC. mPING doesn't record as many severe weather days, particularly outside of the traditional region for large hail east of the Rocky Mountains, with 245 a maximum of only 6 days over central OK and a ridge of activity extending into the Great Lakes 246 region, a broad E-W region over N CO with a weak max roughly over Denver, CO, then a ridge centered roughly over the Appalachians. Through the merger of both sources (Fig. 6b), a more 248 complete picture develops again highlighting their complementary nature. The 20 day maximum 249 over the NE-KS-CO intersection expands, with a clear ridge of frequency extending SE into W 250 OK and the E TX Panhandle. The ridge of severe hail days remains over the Appalachians but 251 likely has a true frequency closer to 8-10 days per year. These patterns are reminiscent of prior 252 climatologies of hail day frequency (Doswell et al. 2005; Allen and Tippett 2015), however also 253 illustrate further regional detail and local maxima.

It is well established that hail displays a strong seasonal cycle with regional variation perhaps even more so than tornado frequency (Changnon Jr 1977; Doswell et al. 2005; Changnon et al. 2009; Allen and Tippett 2015; Taszarek et al. 2020a). To explore these distributions in terms of both sub-severe and severe hail, we explore these characteristics using the seasons as defined from the National Centers for Environmental Prediction, spring (March, April, May), summer (June,

a) Storm Data and mPING Severe Hail Days 2013-2020



b) Combined Storm Data and mPING Severe Hail Days 2013-2020

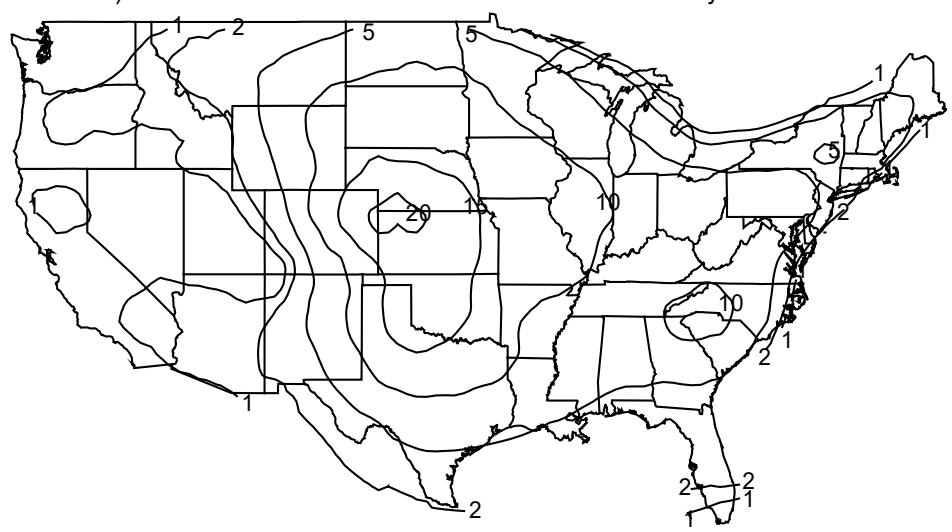


Fig. 6. a) As in Fig. 5a, but for severe hail. b) As in Fig. 5b, but for severe hail.

July and August), fall (September, October, November) and winter (December, January, February), hereafter MAM, JJA, SON and DJF respectively.

Springtime yields the highest frequency for both sub-severe and severe hail over the central Plains (Fig. 7). This broadly consistent with station-based estimates in earlier climatologys (Changnon et al. 2009). Storm Data in contrast produces only about three days of sub-severe hail during an average spring (Fig. 7a), in a rough ellipse extending from NE TX across E OK, into SW MO including the SE corner of KS. Because of Storm Data constraints and aforementioned properties this undercount is expected. The mPING average number of spring sub-severe hail days

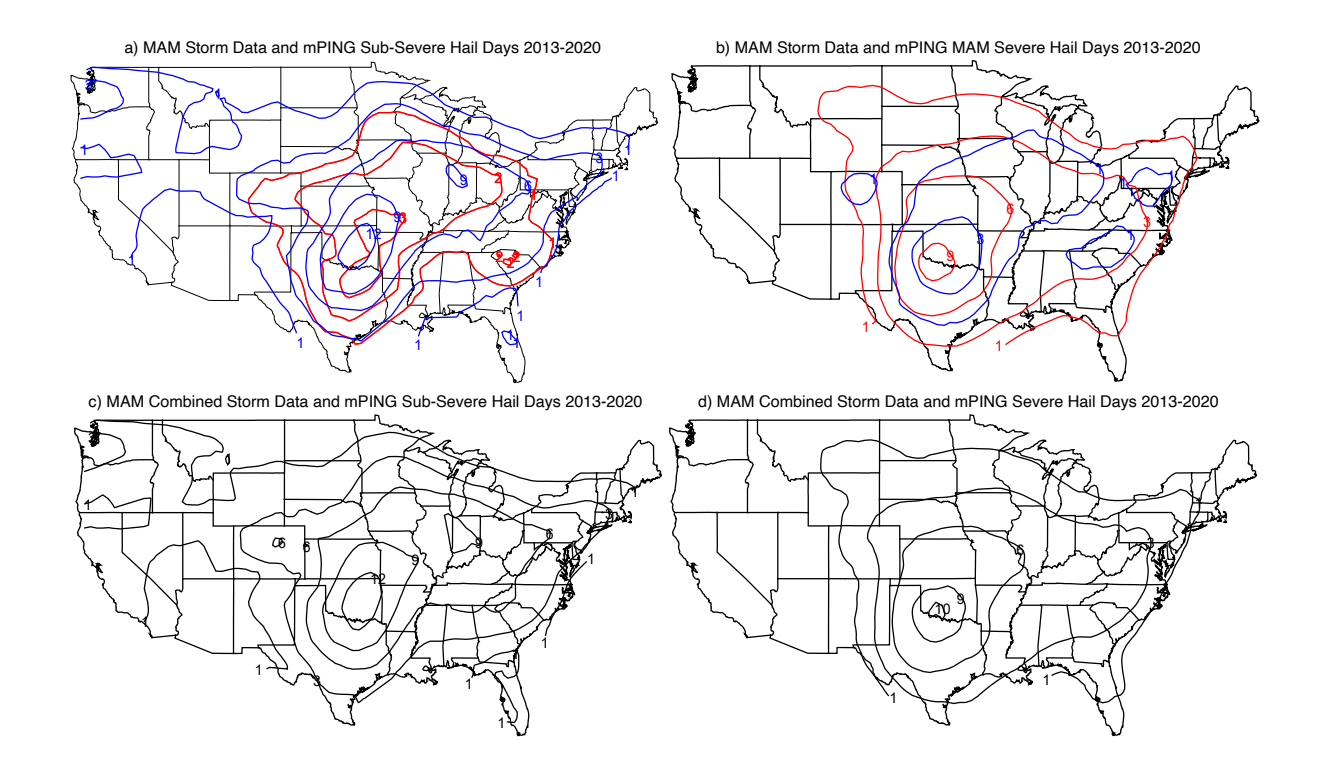


Fig. 7. a) Contours of spring (March, April, May) average number of sub-severe hail days from Storm Data (red) and mPING (blue). b) As for a), but for the spring average number of severe hail days. c) Contours spring average number of sub-severe hail days in spring from both Storm Data and mPING combined. d) As for c), but for the spring average number of severe hail days.

262

263

264

265

capture generally the same spatial pattern for the highest values, but the number of days increase 272 substantially. Higher frequencies also more broadly extend into the Midwest, and minimum contours are more expansive than those of Storm Data. Merging the two sources (Fig. 7c) the 274 pattern is driven primarily by mPING observations. This yields a maximum of 13 days of sub-275 severe hail observations situated over E central OK, extending up into the Great Lakes region then eastward into S New England. There is another maximum (6 days) nestled into the Denver area. 277 For severe hail (Fig. 8c,b), Storm Data days are again more numerous that mPING observations. 278 Here we see maximum average number of days (9 days) shifted slightly to the west and south 279 from the sub-severe days, which is instead centered in southwest OK. A weak ridge of activity extends to the north and east, following roughly the same pattern as for sub-severe hail, but much 281 attenuated. mPING severe hail days are remarkably similar to Storm Data observations, but with 282 fewer observations outside of the traditional hail belt of TX-OK-KS-NE-MO. A non-meteorological

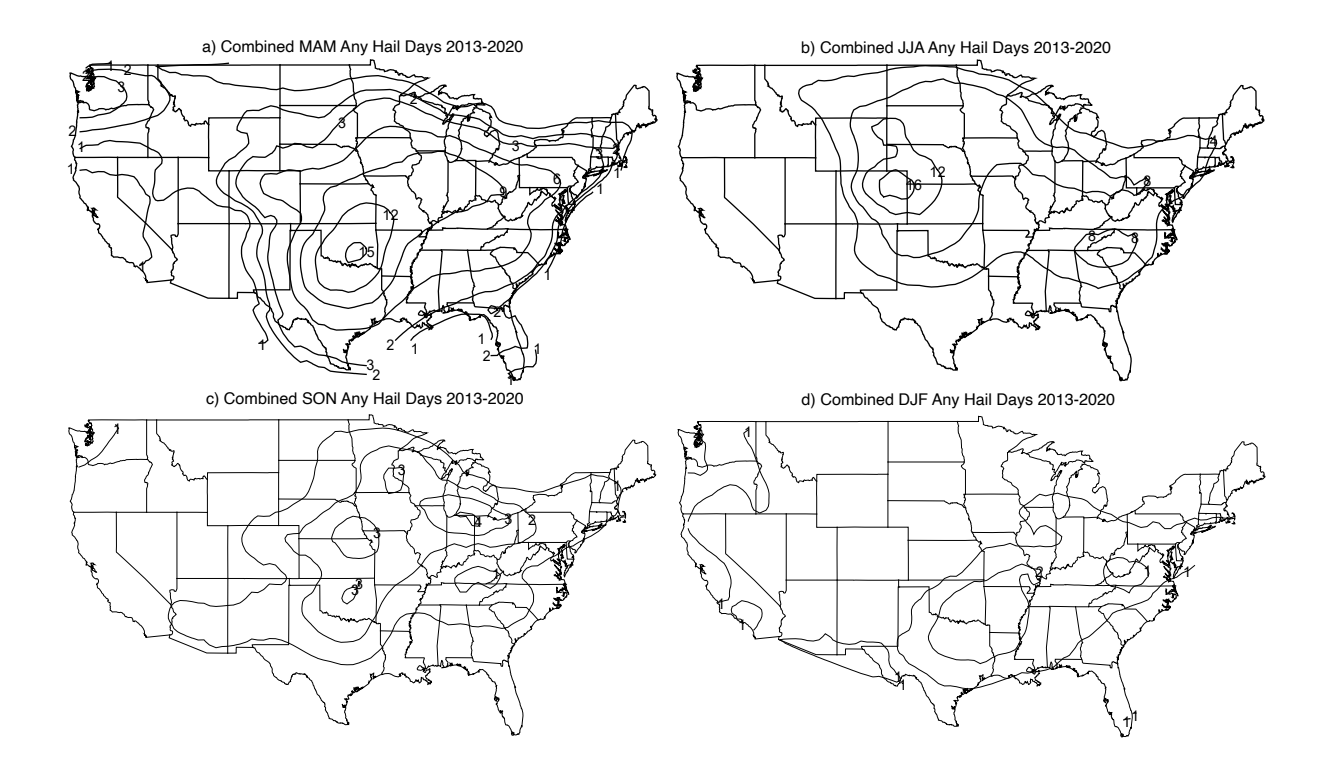


Fig. 8. a) Contours of the spring average number of days with any hail regardless of size from Storm Data and mPING combined regardless of hail size. b) As for a), except for the summer months (June, July, August). c) As for a), except for the fall months (September, October, November), d) As for a), except for the winter (December, January, February).

explanation for this focus may be a function of project familiarity in and around the central OK
area. Finally, merging the two sources (Fig. 7d) the overall pattern is driven by the the larger data
source in Storm Data. The ridge of enhanced activity clearly delineates the expected "hail alley",
along with a broad region of higher frequency extending to the Atlantic coast.

In the summer, sub-severe hail shifts northwards with a broad axis extending from the Rocky Mountains through the Midwest (Fig. 8a). Higher frequencies also extend into the southeastern United States, reflecting weakly forced pulse storms during the summer in this region (Miller and Mote 2017). Storm Data generally undercounts sub-severe hail days and the pattern is significantly different from spring, while mPING sub-severe hail days provide a more coherent depiction. The maximum of eight days is found in the Denver/Ft. Collins, CO area, an extended area of six to seven days from E MN, through the Chicago, IL, area and then through PA. Again, by merging the two data sources (Fig. 8c), we see a more complete picture, with a weak maximum remaining in

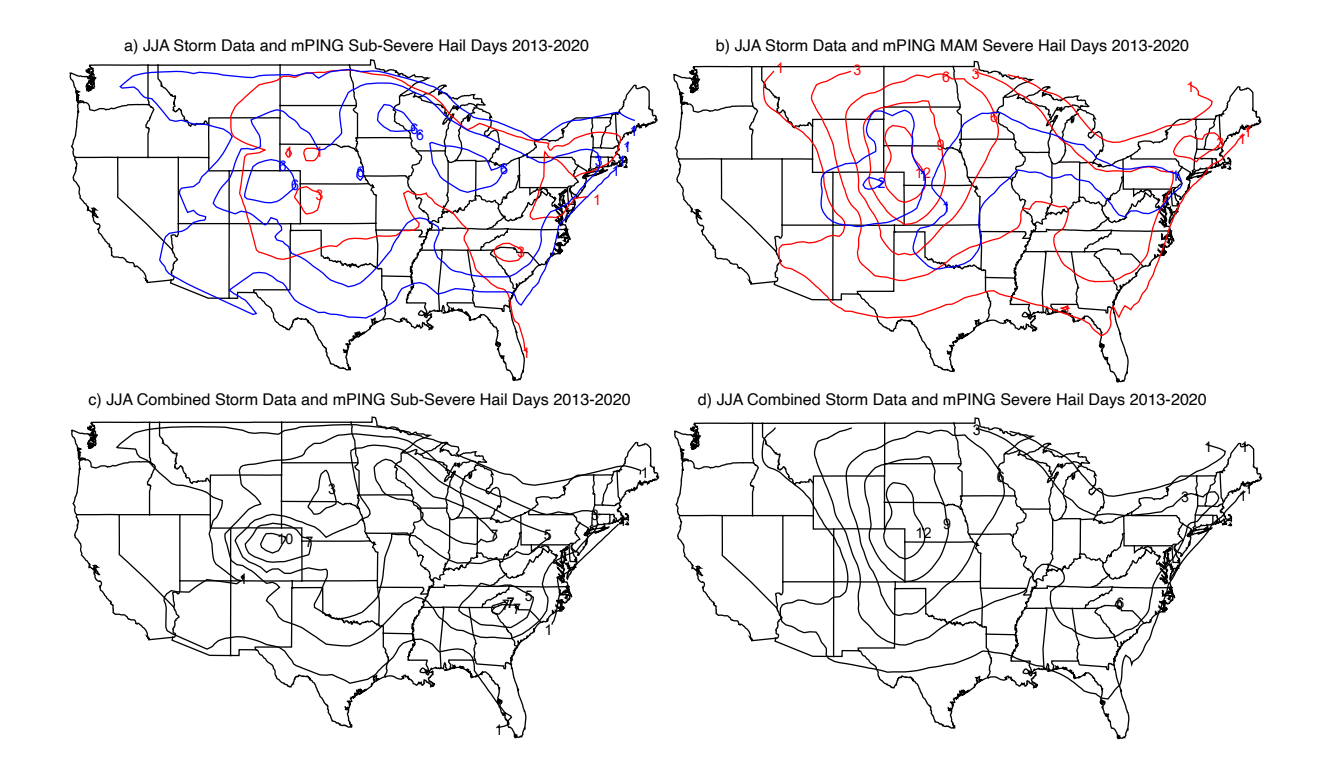


Fig. 9. a) Contours of the yearly average number of sub-severe hail days in summer from Storm Data (red) and mPING (blue). b) As for a), but for severe hail. c) Contours of the yearly average number of sub-severe hail days in summer from both Storm Data and mPING combined. d) As for b) but for severe hail.

C OK, the orographically driven maximum over the Denver area extending into E CO is clearly evident, as is a band of hail activity from eastern Minnesota through the lower Great Lakes and into New England, and a separate maxima is found over the southeast. When only Storm Data severe hail is considered (Fig. 8b), the maximum frequency is clearly centered over NE CO and extends north into western SD, with a broad band of high frequency across the Midwest into the mid-Atlantic. Combining the two datasets results in a broader range of higher frequency severe hail, extending into the northeast (Fig. 8d).

To better illustrate the seasonal progression of occurrence Fig. 9 shows the total hail days, regardless of size, across the seasons from both sources. The average number of winter days with any hail is as would be expected low given limited instability (Fig. 9d). A broad maximum during this season is found over E TX, SE OK, AR, N LA, and S MO. This hints at the maximum in severe weather frequency over the southeast CONUS. Also, on average at least one day of hail occurs along the west Coast, with two days on average in W WA. Frequency rapidly increases into

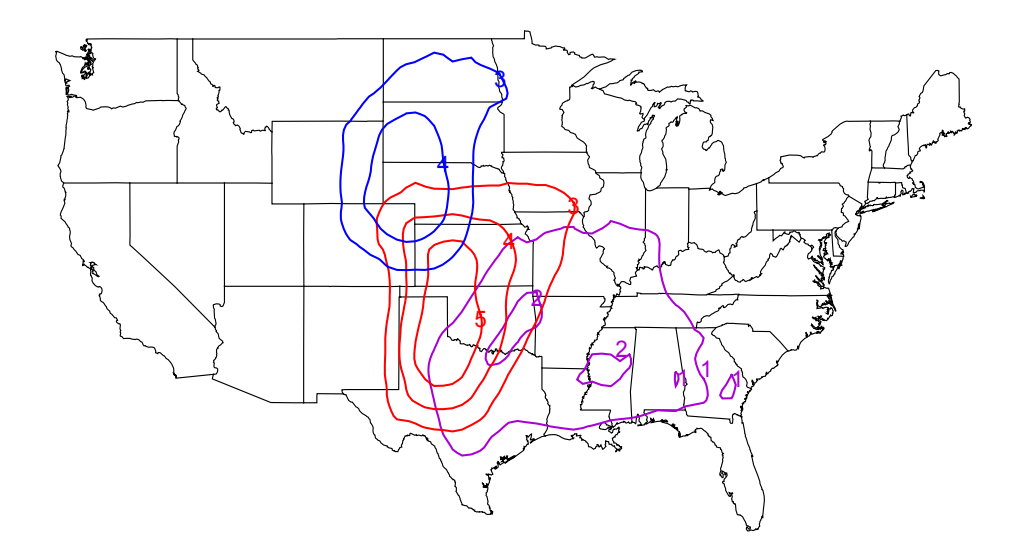


Fig. 10. Contours of the yearly average number days with severe hail for monthly snapshots to illustrate the 328 seasonal cycle in March (purple), May (red) and July (blue). 329

the spring months, with a strong Great Plains signal that extends into the Denver, CO area. Spring however is early in the hail season for many areas closer to the mountains and through the midwest 317 and northeast. During summer maximum surface heating along with convection reach their peak. 318 Two very distinct maxima are identified during the summer for any hail day: one over the Denver area (likely associated with topographic forcing, the "Denver cyclone" (Wilczak and Glendening 320 1988) and the southwest monsoon), and a second maximum over the W NC. The belt of seven to eight days of hail extending from E MN around the Great Lakes through PA becomes more diffuse, but is still evident. Fall sees waning frequency and a lower overall number of days with hail (Fig. 323 9c). Only three days of hail of any size occur and these days all contain a mix of sub-severe and 324 severe hail. On average a broad area of two severe hail days is centered on the KS-NE border (not 325 shown). The main area of hail activity extends from central OK into IA, then eastern MN, curving 326 around the Great Lakes into far western PA. 327

321

330

332

333

Another viewpoint for the seasonal cycle is to consider monthly snapshots through its progression, from March through to May and July (Fig. 10). In March a broad area of severe hail overlays the southeastern CONUS, evidence of the southeastern maximum in severe weather frequency. The number of average severe hail days for May increases, displaying a clear maximum over western OK and the eastern TX panhandle. By July, the frequency maxima extends over the NE panhandle. As has been shown in prior research, the area of peak severe weather progresses west and north from March through July.

b. Hail Size Distribution

Given the distinct differences in the number of sub-severe and severe hail reports between the 338 datasets, a broader examination of the hail size distribution may reveal how these datasets capture 339 the distribution of hail sizes from all reported instances. All reported hail sizes are rounded to the 340 nearest 6.35 mm (0.25"), and a kernel density estimate (KDE) across 201 points using a Gaussian 341 weight 12.7 mm (0.5") wide truncated at four standard deviations of the hail size probability density function estimated. For completeness, the approach here also considers the hail size distribution for 343 the same temporal period (2013-2020) from CoCoRaHS maximum size (when available) reports 344 in comparison to the other two datasets. We choose the maximum size because we suspect that 345 mPING reports also are based on the maximum size observed. Fig. 11 displays the hail size pdfs from all three sources; the missing small sizes are readily apparent in Storm Data. This 347 problematic size distribution has been discussed in prior literature (Allen and Tippett 2015; Allen 348 et al. 2017), with the added influence of clear discontinuities in the pdf associated with the minimum size threshold (0.75 inch), but also the common reference objects used (25.4mm or 1 in, 45mm, or 350 1.75 in Golf Ball, 70mm or 2.75 in Baseball). In comparison, both CoCoRAHS and mPING show 351 a more continuous distribution that includes the smaller sizes, reflecting a more even weighting of frequency toward these categories. Owing to the challenges of Storm Data for understanding the 353 characteristic hail size pdf, we consider a combined pdf of CoCoRaHS and mPING size data (Fig. 354 11). Contrasting the Storm Data pdf, sizes less than 25.4 mm (1 inch) comprise nearly 95 percent 355 of all the 95,009 hail reports (15,169 from CoCoRahs and 79,840 from mPING). This suggests that 356 the use of mPING and CoCoRaHS data combined is a realistic approach to offset the size biases 357 inherent in Storm Data, and these datasets now constitute a record to better explore the occurrence 358 of sub-severe hail and complement the larger sample size of Storm Data. We do however note that CoCoRaHS data may be biased small, as it allows reporting of much smaller sizes leading 360 to differences in the eCDF which imply preferred sizes reported within CoCORaHS that do not 361 appear in mPING. It is also likely that to some extent mPING data may be biased large because the

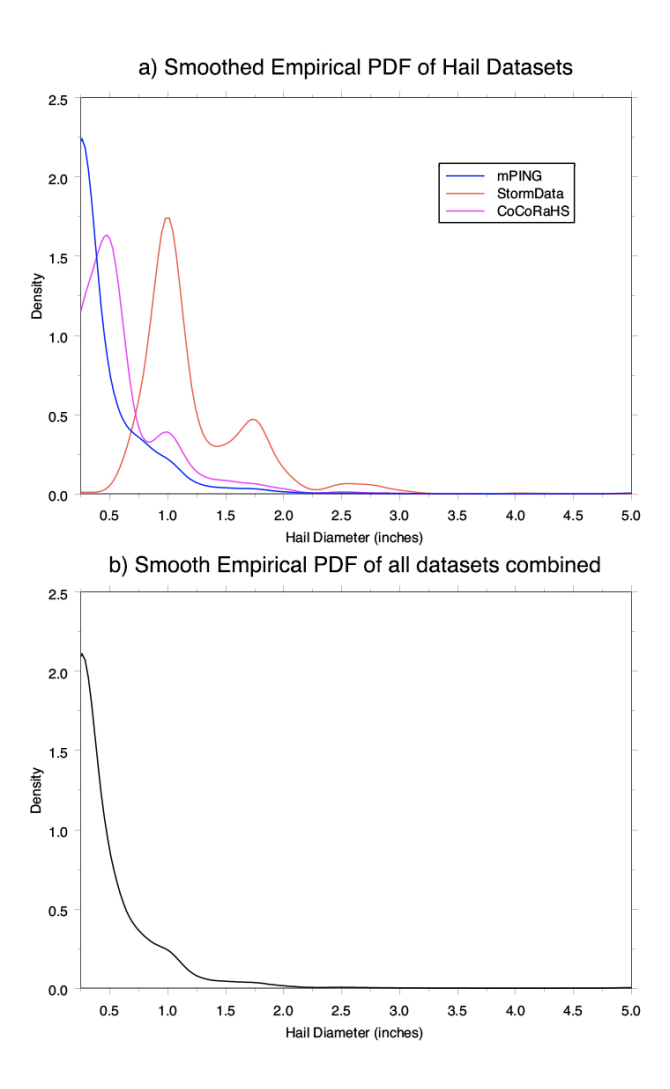


Fig. 11. a) KDE pdfs of hail size for Storm Data (red), mPING (blue) and CoCoRaHS (purple). b) KDE pdfs using combined mPING and CoCoRaHS data.

hail size is estimated rather than measured, and the maximum reporting size of 127mm (5 in) may influence the overall pdf.

367 c. Occurrence Times

369

370

A final climatological aspect of interest is the relative time of occurrence (Fig. 12 a). Transforming hail occurrence time of any size across the respective seasons to LST and applying a KDE, allows exploration of how the temporal structure of hail occurrence varies. We note here that Storm Data occurrence times may on rare occasions be biased late due to observer bias, if the occurrence

time is estimated, and possibly by errors in recording the observation time itself, e.g., recording the submission time rather than the observation time. Even so such errors are rare enough that they do not affect the occurrence time distributions citeportega2021, wendt2021hourly. All seasons show peaks in the late afternoon with relatively slight variations (all times LST): spring at 1630, summer at 1615, fall at 1615, and winter at 1600. These times bracket the peak convective periods that usually follow daytime heating. Variations away from these peaks and spreading of the times away from these peaks may indicate additional effects due to synoptic-scale dynamic processes, a signal highlighted by the higher relative frequencies outside of this peak in winter.

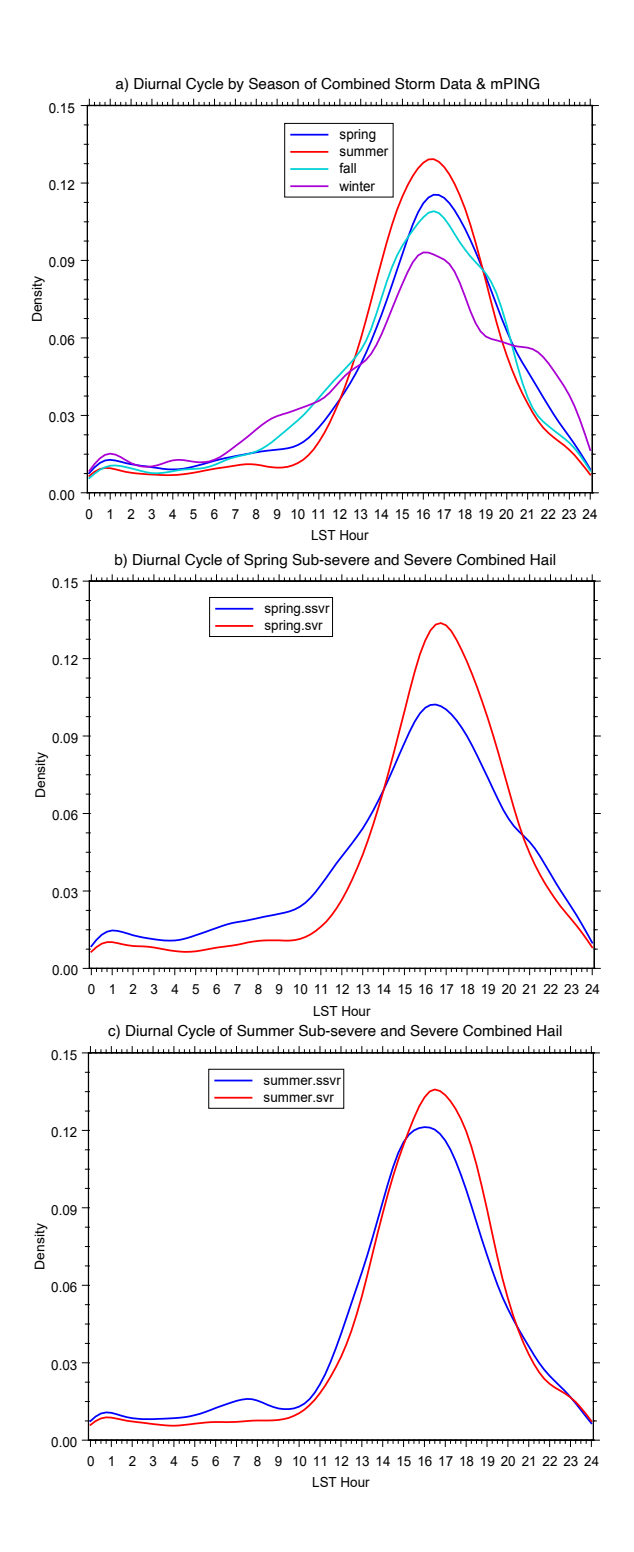


Fig. 12. a) Report/occurrence time in LST of Storm Data and mPING hail events for spring (blue), summer (red), fall (cyan), and winter (magenta). b) Kernel density estimates of report/occurrence times for Storm Data and mPING spring severe hail (red) and sub-severe hail (blue). c) Same as b), but for summer severe (red) and sub-severe (blue).

Seasonally, there are small but discernible differences between the peak times for sub-severe 384 and severe hail (Fig. 12). Two characteristics stand out: the sub-severe peak is at 1630 while the 385 severe peak is on average later in the day at 1645, and the sub-severe peak is more broad than the 386 severe peak is. This is physically consistent as severe hail comes from more energetic convection that likely occurs later in the day possibly in response to greater diabatic heating and the capping 388 inversion's delay of convection (Jewell and Brimelow 2009; Allen et al. 2020; Johnson and Sugden 389 2014; Taszarek et al. 2020b). Sub-severe hail report times are more spread out, possibly indicating that while the convection is strong enough to produce hail, these storms reflect a greater fraction 391 of weakly forced or pulse storms (Miller and Mote 2017), or time frames when convection has 392 weaker vertical updrafts, both earlier in the day and after the nocturnal transition. Differences 393 in the summer are similar: peak report time for sub-severe hail is 1600 while peak report time 394 for severe hail is 1630. The difference is more pronounced and likely reflects the contribution of 395 orographic initiation of thunderstorms earlier in the day, or regions where or pulse thunderstorms 396 are more common but still indicates that the severe reports come later in the day. This also implies that generally speaking sub-severe hail is generated on the periphery of severe convection or to its 398 exclusion. 399

4. Discussion

The exploration of datasets here illustrates that one hail dataset is not superior to another, but 401 rather they approach the characterization of hail occurrence from alternative perspectives and different purposes. In this way, we suggest that the data comprising Storm Data and mPING 403 are complimentary in nature. Through playing to these dataset's relative strengths, we are able 404 to capture a more holistic picture of the hail hazard, similar to the opportunities afforded by station reported records (Changnon and Changnon 2000). By its very design and implementation, 406 Storm Data is clearly the better dataset if the goal is to capture severe hail days. While mPING 407 data expands somewhat on severe hail day numbers, it's primary strength is that it provides a more 408 detailed depiction of smaller, sub-severe hail sizes that Storm Data is not designed to capture. Storm Data is clearly the better dataset if the goal is to capture severe hail days, while mPING data expands 410 on severe hail day numbers, but also provides a more detailed depiction of smaller sub-severe hail 411 sizes. There are other advantages and disadvantages to the respective datasets as well. mPING

reflects a true volunteer and passive collection dataset, capturing whatever observers report. In contrast, Storm Data is biased because in addition to such voluntary reports, the NWS Weather 414 Forecast Offices (WFOs) actively search for severe hail reports (as well as other events) as an 415 approach to verify severe weather warnings (Blair et al. 2011; Bunkers et al. 2020). This can lead to an undersampling bias, or a bias toward the larger hail size as the NWS doesn't continue probing 417 once a warning has been verified (Ortega et al. 2009). Similar to Allen and Tippett (2015), by 418 approaching hail days rather than reports or individual hail events the results presented here are 419 largely unaffected by this characteristic. Curiously, despite relatively widespread coverage mPING 420 severe hail data appears to be a sub-sample of Storm Data. It is true that Storm Data may record 421 sub-severe hail events, but usually this is as an adjunct to some other significant weather event, and 422 since the change of severe criteria in 2010 to 25.4 mm (1 inch), these reports have decreased in 423 frequency (Allen and Tippett 2015). Despite the differences in the total frequency of reports, it is 424 clear that both sources tend to capture similar patterns. 425

While hail, even severe hail, has a relatively common rate of occurrence across the United States it is not commonly observed because of its temporal and spatial heterogeneity and the need to have 427 an observer present (Allen and Tippett 2015). There is no reason to suspect that mPING observers 428 are censoring observations of severe hail, especially since both mPING and Storm Data tend to capture similar spatial patterns, though mPING captures fewer days of severe hail. The likely 430 explanation for this disparity is that the density of mPING observers is not as widespread or as 431 high as the potential sources of reports for Storm Data, both volunteer and solicited. Despite Storm Data not aiming to collect sub-severe hail, there are also pattern similarities that raise an important 433 question about the sub-severe hail days. As mPING is passive, we note that it tends to miss severe 434 hail events by a factor of three to five in comparison to Storm Data. This leads the authors to 435 speculate: is mPING missing the non-severe hail events by the same ratio? If so, the count of sub-severe hail days may be too low by a factor of at least three. Also, within mPING non-severe 437 hail often (but not always) accompanies severe hail observations, though there are clearly days 438 and places when no severe hail is reported but sub-severe hail is. In all likelihood, it is likely that the spatial distribution here underrepresents the frequency of sub-severe hail days, yet the overall 440 pattern of sub-severe hail occurrence is likely well captured. Through analysis and comparison of 441

the sub-severe and severe hail distributions to date using these data, we illustrate that sub-severe hail doesn't always mimic severe hail.

While spatial properties retain some limitations from the sampling, we can ascribe greater 444 confidence for the hail size eCDFs and analysis of hail report times. Both of these metrics are less sensitive to the heterogeneity that can create problems with finding the days with hail. Hail 446 size pdfs indicate that slightly less that five percent of the hail that has been observed over the 447 eight years covered by mPING here meets severe criteria. The remaining record is sub-severe, 448 suggesting that greater attention needs to be paid to exploring how to represent hail days beyond 449 arbitrary severe hail criteria (Doswell 2001), as sub-severe hail can still be damaging to agriculture 450 or lead to large accumulations (Kumjian et al. 2019; Friedrich et al. 2019) that can cause dangerous 451 road conditions and exacerbate flash floods. The diurnal nature of hail reports unsurprisingly lead 452 to an afternoon peak, though clearly if the goal is to sample sub-severe hail, a broader period of 453 observation is necessary. 454

5. Concluding Remarks

Data from three sources (Storm Data, CoCoRaHS, and mPING) over the past eight years have 456 been used to construct a more complete climatology of hail days and characteristics over the 457 CONUS. Differences between these data sources have been discussed to illustrate their relative 458 strengths and applicability, both in combination and individually. Seasonal differences in number of hail days and their spatial distributions have been illustrated, with a spring and summer peak 460 of frequency with a shift of peak from the Southeastern CONUS into the Northwestern Plains, 461 moreso than seen in only severe hail data. Considering sub-severe hail days (days with hail less than 25.4 mm in diameter) and severe hail days, we have shown that there are notable differences 463 in the peaks of hail climatology. Severe hail days also generally record sub-severe hail somewhere, 464 suggesting that the two datasets are not independent. Yet, the spatial distribution of sub-severe hail 465 days differs markedly in some cases from severe hail days.

Considering the reasons for these different depictions, we also explore the size distribution of observed hail through the use of CoCoRaHS, mPING and Storm Data reports. As mPING and CoCoRaHS offer more distributionally complete representations of hail size, we present a combined

eCDF that illustrates the utility of these data to explore the relationship of hail size at the ground to remotely sensed characteristics.

For environmental studies, or other approaches that rely on the time of occurrence we highlighted
the distribution of hail in terms of LST. This analysis reveals differences between sub-severe and
severe hail occurrence of 30 minutes to 1 hour which is much larger than that between seasons,
suggesting that care should be taken when selecting a proximal profile if considering sub-severe
hail environments.

While this work follows on from the depiction of hail occurrence from prior studies (e.g. Kelly 477 et al. 1985; Schaefer et al. 2004; Doswell et al. 2005; Allen and Tippett 2015; Taszarek et al. 478 2020a), it provides a novel insight into the voluntarily sourced small, or sub-severe hail, which has 479 not been directly examined with size information in prior work outside of isolated field datasets. 480 This difference also means that through the use of datasets such as mPING or CoCoRaHS a 481 more comprehensive depiction of hail size distributions is now available to the community. As 482 these datasets continue to grow, this will likely provide a more comprehensive viewpoint of hail occurrence for all sizes offering better opportunities for the validation of radar hail detection, 484 similar to the saturation seen in equivalent approaches in Switzerland (Barras et al. 2019). 485

Despite the advantages, and combination of datasets, the challenges and limitations with observational data remain. Both mPING and CoCoRaHS suffer from the same problems that afflict 487 all other similar observational studies: the uneven spatial distribution of observations. Changnon 488 (1999) pointed to the advantage of fixed station observers for deriving hail frequency which is that, 489 generally speaking these stations reliably identified any hail occurrence in their vicinity. To some 490 extent, this is somewhat less of a problem within Storm Data, particularly in more populated areas 491 of the country, since if no report is received in an area warned for a severe thunderstorm, the NWS 492 WFOs actively probe for verifying observations. The challenge to uncovering a true climatology is that uneven spatial observation distribution cannot be solved by a longer period of record if 494 observations are normalized by area or days as is done here and in other similar studies. The only 495 solution for this problem is to have more observations across a wider array of locations and users. The impacts of spatial inhomogeneity are most easily seen in the difference between the spatial 497 distribution of Storm Data severe hail days as compared to mPING severe hail days. Usually, 498 Storm Data has at least 3X the number of severe hail days that mPING reports, sometimes more.

This difference implies that as diligent as mPING observers are, small hail is probably missed at about the same rate that large hail is missed. Thus do we suspect that there are overall probably 3X as many sub-severe hail days as seen here. While the spatial patterns of sub-severe hail days are likely correct, the frequency remains underestimated.

To offset these limitations remotely sensed climatologies of estimated hail occurrence are now 504 possible (e.g. Cintineo et al. 2012; Murillo et al. 2021; Wendt and Jirak 2021). These technologies 505 are available over a near complete spatio-temporal range for the continent outside of the western CONUS. However, these approaches focus strongly on the maximum expected size of hail, and 507 through lack of appropriate validation data, generally leave sub-severe hail as an afterthought, 508 despite its societal implications. Despite the efforts of projects such as SHAVE (Ortega et al. 2009; Ortega 2018), or those in Switzerland (Barras et al. 2019) a greater volume of sub-severe hail 510 reports is needed to understand the best approach to characterize the total frequency of hail days, 511 the properties of smaller hailstones, and sub-severe hail economic impacts. The question of whether 512 small hail occurrence has changed over time is also a reason to maintain and expand such datasets. For example, over both China and France there have been decreasing trends in smaller hail (Li et al. 514 2016; Sanchez et al. 2017), contrasting the stationary frequency or increases seen for larger hail in 515 the United States (Allen et al. 2015; Tang et al. 2019). With climate projections indicating strong decreases to smaller hail, approaches are needed to monitor these events (Mahoney et al. 2012; 517 Brimelow et al. 2017; Trapp et al. 2019). For mPING and CoCoRAHS to develop into this level of 518 climatological resource likely means that the best approach into the future will be recruitment of additional observers as well as dedicated support. As the observer density increases, fewer events 520 will "slip between the gaps."

- 522 Acknowledgments. Funding was provided for K. Elmore by NOAA/Office of Oceanic
- and Atmospheric Research under NOAA-University of Oklahoma Cooperative Agreement
- #NA21OAR4320204, U.S. Department of Commerce. J. Allen acknowledges funding support
- from the National Science Foundation (AGS-1945286).
- Data availability statement. Observational hail reports from the mPING data are available through
- an API request at https://mping.ou.edu/, with instructions provided for the structuring of
- requests. Storm Data reports for hail for the period can be freely obtained from the Storm
- Prediction Center https://www.spc.noaa.gov/wcm/. CoCoRaHS data are available from
- the project website and use of a web-API request https://www.cocorahs.org/ViewData/
- 531 ListHailReports.aspx.

532 References

- Allen, J. T., I. M. Giammanco, M. R. Kumjian, H. Jurgen Punge, Q. Zhang, P. Groenemeijer,
- M. Kunz, and K. Ortega, 2020: Understanding hail in the Earth system. Rev. Geophysics, 58 (1),
- e2019RG000665.
- Allen, J. T., and M. K. Tippett, 2015: The characteristics of united states hail reports: 1955-2014.
- E-Journal of Severe Storms Meteorology, **10** (3).
- Allen, J. T., M. K. Tippett, Y. Kaheil, A. H. Sobel, C. Lepore, S. Nong, and A. Muehlbauer, 2017:
- An extreme value model for us hail size. *Monthly Weather Review*, **145** (11), 4501–4519.
- Allen, J. T., M. K. Tippett, and A. H. Sobel, 2015: An empirical model relating US monthly
- hail occurrence to large-scale meteorological environment. J. Adv. Modelling Earth Sys., 7 (1),
- 542 226–243.
- Bang, S. D., and D. J. Cecil, 2019: Constructing a multifrequency passive microwave hail retrieval
- and climatology in the GPM domain. J. Appl. Meteor. Climatol., 58 (9), 1889–1904.
- Barras, H., A. Hering, A. Martynov, P.-A. Noti, U. Germann, and O. Martius, 2019: Experiences
- with >50,000 crowdsourced hail reports in Switzerland. Bull. Amer. Meteor. Soc., 100 (8),
- 1429–1440.

- Blair, S. F., D. R. Deroche, J. M. Boustead, J. W. Leighton, B. L. Barjenbruch, and W. P. Gargen,
- ⁵⁴⁹ 2011: A radar-based assessment of the detectability of giant hail. *Electron. J. Severe Storms*
- 550 *Meteorol.*, **6** (**7**).
- Blair, S. F., and Coauthors, 2017: High-resolution hail observations: Implications for NWS warning operations. *Wea. Forecasting*, **32** (3), 1101–1119.
- Brimelow, J. C., W. R. Burrows, and J. M. Hanesiak, 2017: The changing hail threat over North

 America in response to anthropogenic climate change. *Nature Climate Change*, **7** (**7**), 516–522.
- Brooks, H. E., J. W. Lee, and J. P. Craven, 2003: The spatial distribution of severe thunderstorm and tornado environments from global reanalysis data. *Atmos. Res.*, **67-68**, 73–94.
- Brown, T. M., W. H. Pogorzelski, and I. M. Giammanco, 2015: Evaluating hail damage using property insurance claims data. *Wea. Climate Soc.*, **7** (3), 197–210.
- Bunkers, M. J., S. R. Fleegel, T. Grafenauer, C. J. Schultz, and P. N. Schumacher, 2020: Ob-
- servations of Hail-Wind Ratios from Convective Storm Reports across the Continental United
- States. Wea. Forecasting, 35 (2), 635–656, https://doi.org/10.1175/WAF-D-19-0136.1, URL
- https://journals.ametsoc.org/view/journals/wefo/35/2/waf-d-19-0136.1.xml.
- Carr, D. B., A. R. Olsen, and D. White, 1992: Hexagon mosaic maps for display of univariate and
 bivariate geographical data. *Cartography and Geographic Information Systems*, 19 (4), 228–236.
- Cecil, D. J., and C. B. Blankenship, 2012: Toward a global climatology of severe hailstorms as
 estimated by satellite passive microwave imagers. *J. Climate*, 25 (2), 687–703.
- Changnon, D., S. Changnon, and S. Changnon, 2001: A method for estimating crop losses from
 hail in uninsured periods and regions. *J. Appl. Meteor. Climatol.*, **40** (1), 84–91.
- Changnon, D., and S. A. Changnon, 1997: Surrogate data to estimate crop-hail loss. *J. Appl. Meteor.*, **36** (9), 1202–1210.
- Changnon, S. A., 1977: The climatology of hail in North America. *Hail: A review of hail science*and hail suppression, Springer, 107–133.
- ⁵⁷³ Changnon, S. A., 1999: Data and approaches for determining hail risk in the contiguous united states. *Journal of Applied Meteorology*, **38** (**12**), 1730–1739.

- ⁵⁷⁵ Changnon, S. A., and D. Changnon, 2000: Long-term fluctuations in hail incidences in the united states. *Journal of Climate*, **13** (3), 658–664.
- Changnon, S. A., D. Changnon, and S. D. Hilberg, 2009: Hailstorms across the nation: An atlas about hail and its damages. *ISWS Contract Report CR-2009-12*.
- Changnon Jr, S. A., 1971: Hailfall characteristics related to crop damage. *J. Appl. Meteor.*, **10** (**2**), 270–274.
- ⁵⁸¹ Changnon Jr, S. A., 1977: The scales of hail. *J. Appl. Meteor. Climatol.*, **16** (6), 626–648.
- Cintineo, J. L., T. M. Smith, V. Lakshmanan, H. E. Brooks, and K. L. Ortega, 2012: An objective high-resolution hail climatology of the contiguous United States. *Wea. Forecasting*, **27** (5), 1235–1248.
- Cleveland, W. S., 1979: Robust locally weighted regression and smoothing scatterplots. *J. American*Stat Assoc., **74** (**368**), 829–836.
- Cleveland, W. S., and S. J. Devlin, 1988: Locally weighted regression: an approach to regression analysis by local fitting. *J. American Stat Assoc.*, **83 (403)**, 596–610.
- 589 Doswell, C. A., 2001: Severe convective storms—an overview. Severe Convective Storms, 1–26.
- Doswell, C. A., III, H. E. Brooks, and M. P. Kay, 2005: Climatological estimates of daily local nontornadic severe thunderstorm probability for the United States. *Wea. Forecasting*, **20**, 577–592 595, https://doi.org/10.1175/WAF866.1.
- Elmore, K. L., Z. Flamig, V. Lakshmanan, B. Kaney, V. Farmer, H. D. Reeves, and L. P. Rothfusz, 2014: mping: Crowd-sourcing weather reports for research. *Bull. Amer. Meteor. Soc.*, **95** (9), 1335–1342.
- Friedrich, K., and Coauthors, 2019: Chat: The Colorado Hail Accumulation from Thunderstorms project. *Bull. Amer. Meteor. Soc.*, **100** (3), 459–471.
- Gensini, V. A., A. M. Haberlie, and P. T. Marsh, 2020: Practically perfect hindcasts of severe convective storms. *Bull. Amer. Meteor. Soc.*, **101** (8), E1259–E1278.

- 600 Giammanco, I. M., B. R. Maiden, H. E. Estes, and T. M. Brown-Giammanco, 2017: Using 3D
- laser scanning technology to create digital models of hailstones. Bull. Amer. Meteor. Soc., 98 (7),
- 1341-1347.
- ⁶⁰³ Grieser, J., and M. Hill, 2019: How to express hail intensity—modeling the hailstone size distri-
- bution. J. Appl. Meteor. Climatol., **58** (**10**), 2329–2345.
- Jewell, R., and J. Brimelow, 2009: Evaluation of alberta hail growth model using severe hail
- proximity soundings from the united states. Wea. Forecasting, **24**, 1592–1609.
- Johnson, A. W., and K. Sugden, 2014: Evaluation of Sounding-Derived Thermodynamic and Wind-
- Related Parameters Associated with Large Hail Events. *E-Journal of Severe Storms Meteorology*,
- 9 (5), 1–42, URL http://www.ejssm.org/ojs/index.php/ejssm/article/viewArticle/137.
- Kacan, K. G., and Z. J. Lebo, 2019: Microphysical and dynamical effects of mixed-phase hydrom-
- eteors in convective storms using a bin microphysics model: Melting. *Monthly Weather Review*,
- 147 (12), 4437–4460.
- Kelly, D. L., J. T. Schaefer, and C. A. Doswell III, 1985: Climatology of nontornadic severe
- thunderstorm events in the united states. *Monthly Weather Review*, **113** (**11**), 1997–2014.
- Kumjian, M. R., Z. J. Lebo, and A. M. Ward, 2019: Storms producing large accumulations of
- small hail. J. Appl. Meteor. Climatol., **58** (2), 341–364.
- Li, M., Q. Zhang, and F. Zhang, 2016: Hail day frequency trends and associated atmospheric
- circulation patterns over China during 1960–2012. *J. Climate*, **29** (**19**), 7027–7044.
- Mahoney, K., M. A. Alexander, G. Thompson, J. J. Barsugli, and J. D. Scott, 2012: Changes in
- hail and flood risk in high-resolution simulations over Colorado's mountains. *Nature Climate*
- 621 Change, **2** (**2**), 125–131.
- Miller, P. W., and T. L. Mote, 2017: A climatology of weakly forced and pulse thunderstorms in
- the southeast United States. J. Appl. Meteor. Climatol., **56** (11), 3017–3033.
- Murillo, E. M., C. R. Homeyer, and J. T. Allen, 2021: A 23-year severe hail climatology using
- 625 GridRad MESH observations. *Mon. Wea. Rev.*, **149** (4), 945–958.

- Ortega, K. L., 2018: Evaluating multi-radar, multi-sensor products for surface hailfall diagnosis.
- E-Journal Sev. Storms Meteorol, 13 (1).
- Ortega, K. L., T. M. Smith, K. L. Manross, K. A. Scharfenberg, A. Witt, A. G. Kolodziej, and J. J.
- Gourley, 2009: The severe hazards analysis and verification experiment. Bull. Amer. Meteor. Soc.,
- **90 (10)**, 1519–1530.
- Reges, H. W., N. Doesken, J. Turner, N. Newman, A. Bergantino, and Z. Schwalbe, 2016: Cocorahs:
- The evolution and accomplishments of a volunteer rain gauge network. *Bull. Amer. Meteor. Soc.*,
- **97 (10)**, 1831–1846.
- Sanchez, J., A. Merino, P. Melcón, E. García-Ortega, S. Fernández-González, C. Berthet, and
- J. Dessens, 2017: Are meteorological conditions favoring hail precipitation change in Southern
- Europe? Analysis of the period 1948–2015. *Atmos. Res.*, **198**, 1–10.
- Sander, J., J. Eichner, E. Faust, and M. Steuer, 2013: Rising variability in thunderstorm-related US
- losses as a reflection of changes in large-scale thunderstorm forcing. Wea. Climate Soc., 5 (4),
- 639 317–331.
- Schaefer, J. T., J. J. Levit, S. J. Weiss, and D. W. McCarthy, 2004: The frequency of large hail over
- the contiguous United States. Preprints, 14th Conf. on Applied Climatology, Seattle, WA, Amer.
- Meteor. Soc, Citeseer, Vol. 3.
- 643 Silverman, B. W., 1998: Density estimation for statistics and data analysis. Routledge, 176 pp.
- Tang, B. H., V. A. Gensini, and C. R. Homeyer, 2019: Trends in United States large hail environ-
- ments and observations. NPJ Clim. Atmos, Sci., 2 (1), 1–7.
- Taszarek, M., J. T. Allen, P. Groenemeijer, R. Edwards, H. E. Brooks, V. Chmielewski, and S.-E.
- Enno, 2020a: Severe convective storms across Europe and the United States. Part I: Climatology
- of lightning, large hail, severe wind, and tornadoes. J. Climate, 33 (23), 10 239–10 261.
- Taszarek, M., J. T. Allen, T. Púčik, K. A. Hoogewind, and H. E. Brooks, 2020b: Severe convective
- storms across europe and the united states, part ii: Era5 environments associated with lightning,
- large hail, severe wind, and tornadoes. *Journal of Climate*, **33 (23)**, 10 263–10 286.

- Trapp, R. J., K. A. Hoogewind, and S. Lasher-Trapp, 2019: Future changes in hail occurrence in the United States determined through convection-permitting dynamical downscaling. *J. Climate*, 32 (17), 5493–5509.
- Van Den Heever, S. C., and W. R. Cotton, 2004: The impact of hail size on simulated supercell storms. *Journal of the atmospheric sciences*, **61** (**13**), 1596–1609.
- Wendt, N. A., and I. L. Jirak, 2021: An hourly climatology of operational MRMS MESH-diagnosed severe and significant hail with comparisons to Storm Data hail reports. *Wea. Forecasting*, **36** (2), 645–659.
- Wilczak, J. M., and J. W. Glendening, 1988: Observations and mixed-layer modeling of a terrain induced mesoscale gyre: The denver cyclone. *Mon. Wea. Rev.*, 116, 1599–1622.
- Witt, A., M. D. Eilts, G. J. Stumpf, E. D. W. Mitchell, J. Johnson, and K. W. Thomas, 1998:
 Evaluating the performance of WSR-88D severe storm detection algorithms. Wea. Forecasting,
 13 (2), 513–518.